energies

MDPI

Article

Mechanical Response of Geopolymer Foams to Heating—Managing Coal Gangue in Fire-Resistant Materials Technology

Mateusz Sitarz [1], Beata Figiela [2], Michał Łach [2], Kinga Korniejenko [2], Katarzyna Mróz [1], João Castro-Gomes [3] and Izabela Hager [1,*]

[1] Chair of Building Materials Engineering, Faculty of Civil Engineering, Cracow University of Technology, 24 Warszawska Street, 31-155 Cracow, Poland; mateusz.sitarz@pk.edu.pl (M.S.); katarzyna.mroz@pk.edu.pl (K.M.)
[2] Chair of Materials Engineering, Faculty of Material Engineering and Physics, Cracow University of Technology, 37 Jana Pawła II Street, 31-864 Cracow, Poland; beata.figiela@pk.edu.pl (B.F.); michal.lach@pk.edu.pl (M.Ł.); kinga.korniejenko@pk.edu.pl (K.K.)
[3] Centre of Materials and Building Technologies (C–MADE), Department of Civil Engineering and Architecture, University of Beira Interior (UBI), 6201-001 Covilhã, Portugal; jpcg@ubi.pt
* Correspondence: izabela.hager@pk.edu.pl; Tel.: +48-12-628-23-67

Abstract: Two geopolymer foams were prepared from a thermally activated coal gangue containing kaolinite. As the foaming agent, aluminium powder and 36% hydrogen peroxide were used to obtain two levels of porosity. The materials' high temperature performances were investigated: tensile and compressive strength evolution with temperature. This study shows that the mechanical performances of developed geopolymer foams are similar to foam concrete of the same apparent density. The geopolymer foams from coal gangue present stable mechanical performances up to 600 °C. When the glass transition temperature is achieved, sintering occurs and mechanical performance increases. SEM observations confirm the glass transition and densification of the matrix at temperatures above 800 °C. Moreover, the XRD measurements revealed a high amount of mullite that forms at 1000 °C that explained the observed strength increase. The synthesis of good-quality geopolymer foams from coal gangue and its application as a thermal barrier is feasible. The constant level of porosity and its stable character in the range of temperatures 20–1000 °C ensures stable thermal insulation parameters with increasing temperature, which is extremely important for fire protection.

Keywords: geopolymers; coal gangue; high temperature; mechanical performances

Citation: Sitarz, M.; Figiela, B.; Łach, M.; Korniejenko, K.; Mróz, K.; Castro-Gomes, J.; Hager, I. Mechanical Response of Geopolymer Foams to Heating—Managing Coal Gangue in Fire-Resistant Materials Technology. *Energies* **2022**, *15*, 3363. https://doi.org/10.3390/en15093363

Academic Editor: F. Pacheco Torgal

Received: 26 March 2022
Accepted: 29 April 2022
Published: 5 May 2022

1. Introduction

The first application of geopolymers in the construction industry was developed in 1973–1976 as fire-resistant chipboard [1,2]. It consisted of a wooden core covered with two geopolymer coatings. The entire panel was produced in a single-step process [2,3]. The investigation in the next years confirmed good fire resistance up to 1000 °C [4]. Nowadays, the area of applications of geopolymers in high temperature is one of the most promising ways for their application, including some existing market products such as Nu-Core® A2FR (geopolymer composite panels), Ino-Flamm® (fire-resistant geopolymer paint) and SKOBI-FIX 30 (geopolymer foam dedicated for heating systems) [5].

In the case of geopolymers, especially based on metakaolin and fly-ash, relatively large works connected with the behaviour of these materials at elevated temperatures has been conducted [4,6]. This investigation includes fire resistance, as well as temperature resistance of these materials, including the influence of temperature on mechanical properties [6,7]. The research was provided for pure geopolymer matrix [8,9], and also for composites reinforced by different types of fibres, such as carbon [10–12], basalt [10,13], polymer [8,14] and

natural fibres [15–17]. The results obtained by the researchers show different behaviours for these types of materials; while some researchers report a decrease in the mechanical properties of materials with temperature [11], others report an increase. For example, Shaikh and Haque [10] noticed an increase in the mechanical properties of geopolymer composites reinforced by fibres at temperatures of 200 °C, 400 °C, and 600 °C compared with the materials tested at an ambient temperature of 28 °C, but decreasing the values in 800 °C. Behera et al. [12] observed a decrease in mechanical properties (compressive and tensile strength) up to 200 °C. Tayeh et al. [18] noticed decreasing compressive strength for temperatures above 100 °C. However, the trials of composition coherent model the behaviour for geopolymers in elevated temperature are undertaken; they do not provide sufficient explanation for all phenomena that appeared during the research [3,6].

In the case of foamed materials, only a few investigations in this area have been carried out [19,20]. The general observed tendency is that, compared to plain geopolymers, foamed geopolymers have better strength retention at elevated temperatures [21,22]. This is probably caused by better vapour and heat transfers in porous structures, which minimises thermo-mechanical stress [21,22]. Most research has been conducted on metakaolin or fly ash-based geopolymers at temperatures up to 800 °C [22,23]. This investigation shows that fly ash- and metakaolin-based geopolymers usually show better mechanical properties at elevated temperatures compared to slags [22]. Research on foamed geopolymers shows a decrease in mechanical properties with an increasing temperature of up to 800 °C [21,24]. Above this temperature, a limited number of investigations have been conducted. Some of them show that the mechanical properties of geopolymers could increase due to sintering and skeleton solidification [22,25,26].

This study analyses the mechanical properties of foamed waste-based geopolymers. The raw material for the geopolymer was the gangue from coal mine Wieczorek (Poland), mainly composed of quartz and aluminosilicates in the form of minerals, such as kaolinite and illite. Gangue is a commercially worthless material. It is the waste rock overlying an ore that needs to be displaced during the mining process. These mine tailings need to be managed and appropriately processed. The possible waste management of this type of tailing in building materials was found to be beneficial for the environment. The main novelty of this research is the investigation of the possibility of using this waste stream in fire-resistant foamed panels.

The foamed geopolymer with high total porosity, low density and limited thermal conductivity is an excellent thermal insulator. It is considered that the properties of foamed geopolymer, its strength and modulus elasticity decrease with density. The mineral skeleton of geopolymers is non-flammable, fire-resistant and stable in high-temperature applications. Moreover, it is highly vapour-permeable due to its porous structure. The parameters of interest to the authors are their satisfactory thermal insulation and fire resistance at the Euroclass A1—the highest resistance class due to the lack of organic particles and compounds.

The investigation was carried out to observe the evolution of mechanical performance compressive and flexural tensile strength at temperatures up to 1000 °C. The visual aspects, density, apparent density and porosity were determined. Moreover, microstructural observations and EDS analysis were undertaken. The main goal was to provide data on the mechanical response of the material to heating. The behaviour of this material was commented on in the context of a previous investigation of foamed geopolymers based on metakaolin and fly ash, because of the lack of previous research on foamed geopolymers based on mine tailings for this application and range of temperature.

2. Materials and Methods

Foam geopolymer samples were produced based on waste material from a Wieczorek coal mine (Poland). The coal mine tailings still represent a significant waste stream in Poland. Figure 1 and Table 1 show the percentage of identified phases using X-ray diffraction on a PANanalitycal Almelo at material from Wieczorek Mine. The test was carried out

on a powdered material using a Cu lamp. Analysis of the identified phases was performed with the use of High Score Plus software. The study showed the presence of such minerals in the material as: quartz—50%, kaolinite—28.2%, illite—14.3% and muscovite—7.5% (Table 1).

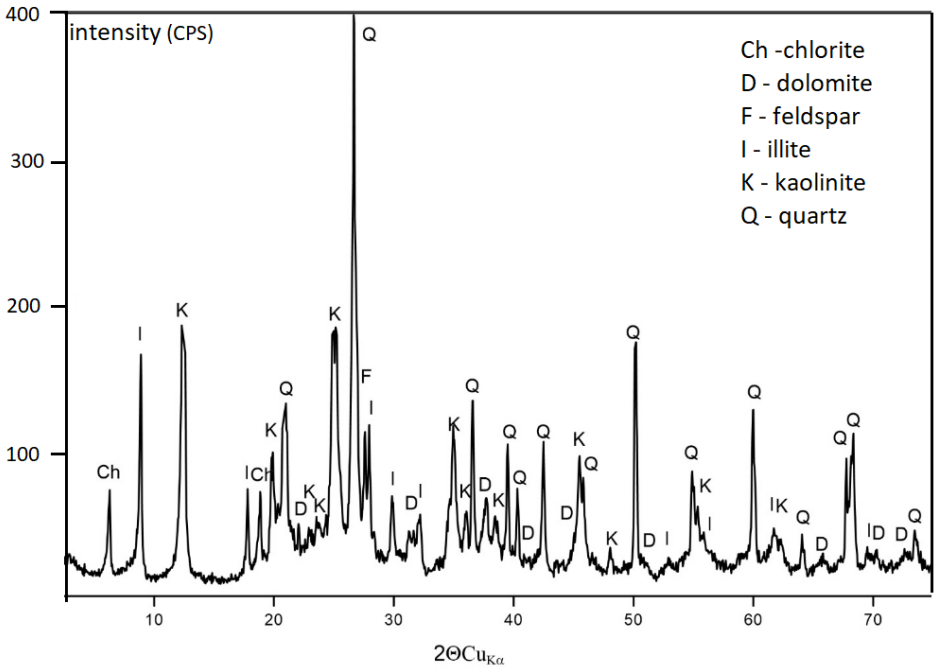

Figure 1. XRD of coal gangue from Wieczorek coal mine. On the *y*-axis, the relative intensity of the diffracted beam.

Table 1. Percentage of identified minerals in gangue from the Wieczorek mine.

Sample	Identified Mineral		Percentage [%]
	Name	Chemical Formula	
coal gangue from Wieczorek mine	quartz	SiO_2	50.0
	muscovite-2M1	$KAl_2(Si_3Al)O_{10}(OH,F)_2$	7.5
	kaolinite-1Ad	$Al_2Si_2O_5(OH)_4$	28.2
	illite-2M1	$(KH_3O)Al_2Si_3AlO_{10}(OH)_2$	14.3

The coal gangue from the mine was first crushed due to the large size of the coal shale and then mechanically ground to a particle size below 750 µm. The powder obtained was subjected to thermal treatment: heating for 24 h at 700 °C. This thermal treatment enabled the calcination of mineral compounds, increasing the reactivity of the material, leading to the formation of highly reactive precursors for geopolymerisation, also reducing the carbon content. The loss of ignition was 5.2% LOI. In the calcinated gangue, no coal or any organic components were present in the composition of developed geopolymer foams. The XRF tests enabled the identification of calcinated coal gangue oxide composition expressed in % of total mass of the sample (Table 2).

A 10 M sodium hydroxide solution with aqueous sodium silicate was used as an activator for the production of geopolymer foams. The solution was made of flakes of technical sodium hydroxide (from PCC ROKITA S. A.) mixed with tap water conform with [27], to which was then added sodium water glass type R-145, density 1.45 g/cm^3, MR > 1.6 (from CHEMI KAM Sp. z o.o.) in a ratio of 1:2.5. All ingredients were mixed thoroughly, and the solution was allowed to equilibrate in concentration and temperature for 24 h.

Table 2. Identified oxide composition of calcinated coal gangue from the Wieczorek mine by the XRF method.

Compound Formula	Conc. (%)
SiO_2	63.925
Al_2O_3	23.839
Fe_2O_3	4.699
K_2O	2.561
MgO	1.864
TiO_2	0.986
Na_2O	0.813
SO_3	0.429
CaO	0.233
P_2O_5	0.115
Cr_2O_3	0.113
MnO	0.056
CeO_2	0.055
NiO	0.037
ZrO_2	0.028
BaO	0.026
Co_3O_4	0.014
Rb_2O	0.012

Powdered aluminium from R & G GmbH and 36% hydrogen peroxide from Chempur were used as foaming agents for geopolymers. Thirty-six percent hydrogen peroxide contains H_2O_2 (molar mass 34.01 g/mol, density—1.133 g/mL). They are the two most commonly used foaming agents in cementitious and geopolymer materials [28,29]. The preliminary results of the trial bathes led us to conclude that the best effect in foaming this type of geopolymer is the use of a mix of H_2O_2 and aluminium powder.

A weighted amount of the ingredients was placed in the bowl of a low-speed mixer and the previously prepared solution was added. All components were mixed for 15 min, and then 36% hydrogen peroxide, along with a portion of aluminium powder and hydroxyethyl cellulose stabiliser (from Glentham Life Sciences, Corsham, UK) were added (Table 3). Al-1 contained 0.15% aluminium powder and 0.3% cellulose stabiliser and Al-2 contained 0.3% aluminium powder and the same amount of cellulose stabiliser as Al-1 (0.3%). In both materials, there was the same amount of hydrogen peroxide—0.75%.

Table 3. Composition of foamed geopolymer mixes.

Sample	Precursor	Foaming Agent		Stabiliser
	Calcinated Wieczorek Coal Gangue	Aluminium Powder	36% Hydrogen Peroxide	Hydroxyethyl Cellulose
Al-1	98.8%	0.15%	0.75%	0.3%
Al-2	98.7%	0.30%	0.75%	0.3%

The aerated paste prepared in this way was cast into a set of 40 mm × 40 mm × 160 mm prismatic moulds. Then, the mould sets were placed in a laboratory dryer to the temperature of 75 °C for 24 h. After this time, the samples were cooled to ambient temperature, unmoulded and seasoned for 28 days to perform the tests.

The material density was determined using a helium pycnometer ULTRAPYCTOMETR 1000, Quantachrome. The apparent density was determined by the geometrical method using an electronic calliper (measuring accuracy up to 0.01 mm) and a RADWAG analytical balance with a measurement accuracy of 0.001/0.01 g. The values of total porosity were evaluated based on density and apparent density values.

The samples were heated in the Nabertherm furnace with a heating rate of 1°C/min, to temperature 200, 400, 600, 800 and 1000 °C. This heating rate follows RILEM recommendations [30] to minimise stress due to temperature differences between hotter surfaces and cooler inner parts of the sample. These heating conditions are considered to be adequate to evaluate the influence of temperature impact on concrete and other mineral materials such as geopolymers and were previously used in [31–33]. When the set temperature from range 200–1000 °C has been achieved, it was maintained for 1 h to homogenise the temperature in the entire cross-section of the sample.

After cooling down the specimens in the furnace, the appearance and structure conditions were observed. The foam sample pictures were taken under constant lighting conditions. Recently, the author proposed a technique [34] to study the colour change of concrete due to heating. For this purpose, a flatbed scanner (HP Scanjet) was used to obtain constant lighting conditions while pictures of concrete samples were taken. No expensive measurement equipment and/or colour analysis computer software is necessary to perform these observations. The colour analysis was performed using an open access image analysis software package (Scion Image).

After cooling the 40 × 40 × 160 mm samples down, each was tested in a three-point bending test using a Controls testing machine. The loading rate applied was 50 N/s. The remaining prisms (40 × 40 × aprox. 80 mm) produced by bending tests were used to determine compressive strength. The load was applied at a loading rate of 2400 N/s.

All the tested mechanical and physical features were referenced to the 20 °C values obtained for the unheated samples. The relative changes in the tested properties, as well as the changes in material structure, were determined and represented in the figures.

The scanning electron microscope (SEM) images were taken using a JEOL JSM-IT200 with the scanning electron microscope (JEOL, Tokyo, Japan). Crushed material after the tests was stuck onto carbon tape. The samples were coated with a layer of gold to ensure good conductivity using a DII-29030SCTR Smart Coater (JEOL, Tokyo, Japan).

3. Results

3.1. Visual Aspect and Colour Change of the Heated Foams

The visual aspect of the sample's surface is presented in Figure 2. Two foams were obtained with two levels of powdered aluminium addition, Al-1 and Al-2. The difference in structure and porosity is represented in Figure 1, where the specimens' surface after demoulding and porosity visible on the cross-section was depicted. The double aluminium powder content did not significantly increase the number of pores in the material but induced the porosity type, size and pore distribution.

The sample surface of Al-1 was significantly different from Al-2, so we clearly distinguished large pores for Al-1. The surface of the Al-2 sample presented a characteristic wall effect—the geopolymer paste concentrated near the mould wall. On the cross-section, we observed that Al-1 had a significant number of big pores. The pore sizes varied; we had large pores, up to 5 mm, as well as large amounts of fine pores. In the case of Al-2, the distribution of pores and their sizes were more uniform (see Figure 2).

The visual aspect of the sample's surface after heating is shown in Figures 3 and 4, where the colour change is represented. As a result of heating, a progressive colour change was observed. A pinkish colouration was noted after heating to 600 °C, in all the samples. The red colourations were more pronounced after 1000 °C where the effect of iron compound oxidation was most pronounced. For the samples heated to 1000 °C, their bending was due to more intense shrinkage resulting from sintering (Figures 3 and 4). The contraction was more intense in the bottom part of samples, where more dense and less porous material was placed, and the shrinkage was more pronounced. After heating, the samples were inspected to observe any defects or chipping. None of the samples were damaged during heating. The samples' integrity after heating was maintained for both compositions Al-1 and Al-2.

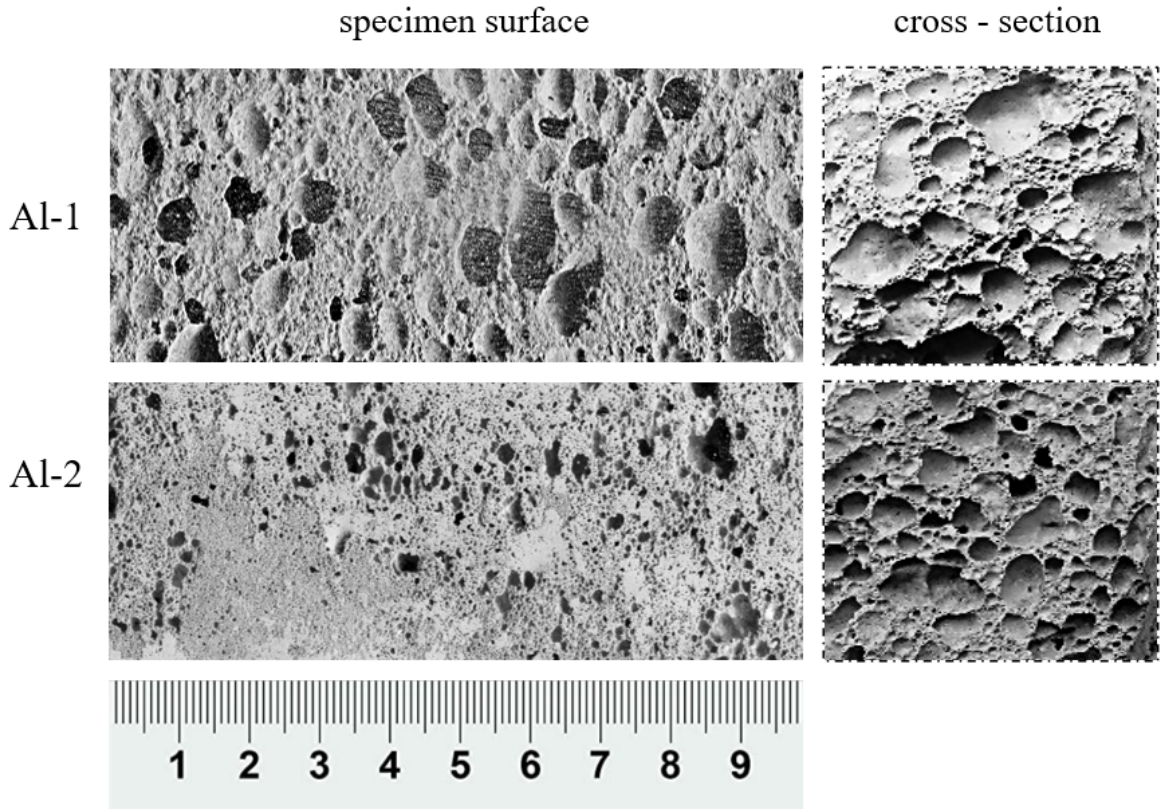

Figure 2. Surface and cross-section of the samples—porous structure and pores arrangement.

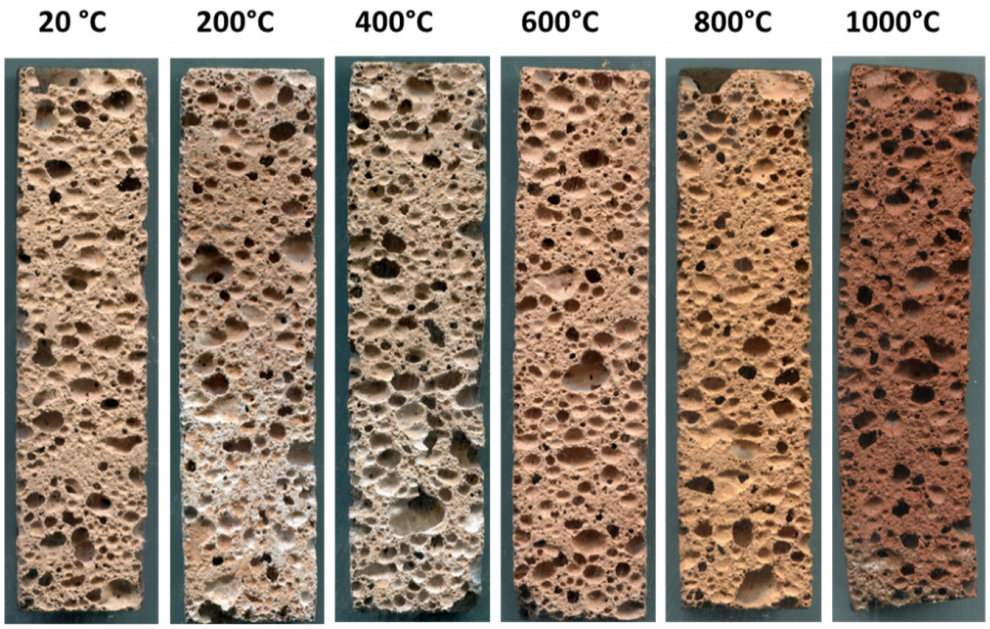

Figure 3. Visual aspect and colour change in heated geopolymer foam Al-1.

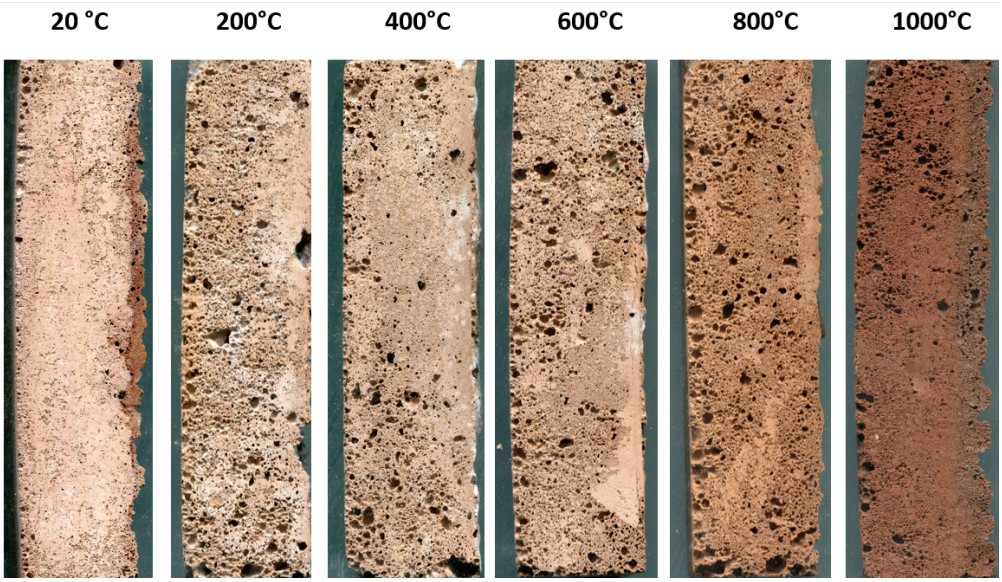

Figure 4. Visual aspect and colour change in heated geopolymer foam Al-2.

3.2. Apparent Density, Density and Porosity of Heated Foams

The apparent densities of unheated material were 615 ± 60 kg/m^3 Al-1 and 835 ± 50 kg/m^3 for Al-2, and their true densities evaluated with a helium pycnometer were 3021.3 kg/m^3 and 2840.2 kg/m^3 (Figure 5). Samples containing a double portion of powdered aluminium (Al-2) had a slightly higher apparent density, despite a higher amount of aluminium powder. The expected porosity increase was not observed. The evaluated total porosities reflected this observation. The porosity of Al-1 was 80% and that of Al-2 was 70% (Figure 6). The lower-than-expected porosity of Al-2 may be due to the too low content of the compounds reactive with aluminium oxide in the precursor, releasing hydrogen, which forms porosity in the geopolymer structure. The lower density of Al-1 was attributed to a more significant number of pores in the material and their larger size, as shown in the cross-section presented in Figure 1.

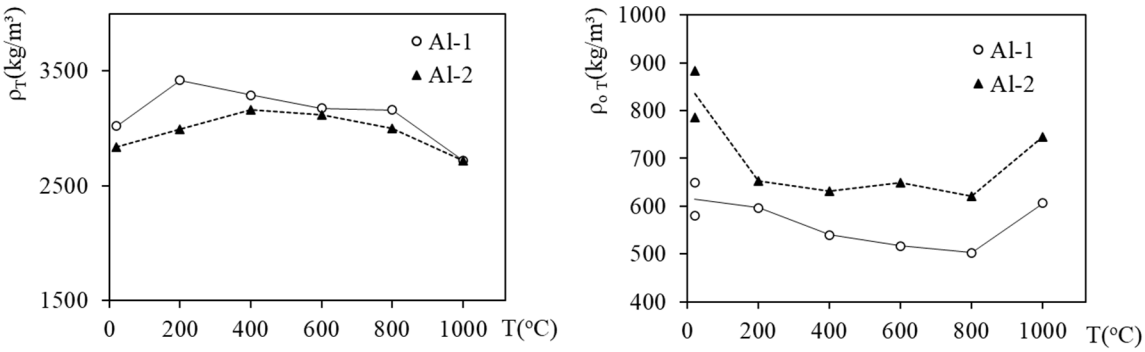

Figure 5. Density ρ and apparent density ρ_o in kg/m^3 of heated geopolymer foams.

When heated, the apparent density of foams slightly decreased due to the matrix and aggregate drying. The moisture contained in the material was gradually removed by heat. This resulted in a slight density decrease at 200 °C. Further heating did not significantly affect the apparent density change. At higher temperatures, the physically bound water evaporated, and the hydroxyl groups were removed. Some sources point out that the process of dehydroxylation starts at 250 °C and continues up to 600 °C [31], which induces shrinkage of the geopolymer binder. An increase in density after exposure to 800 °C was due to shrinkage and matrix densification related to the sintering process. The relatively

high amount of alkalis led to a glass transition that started at approximately 700 °C and recrystallisation of melting phases.

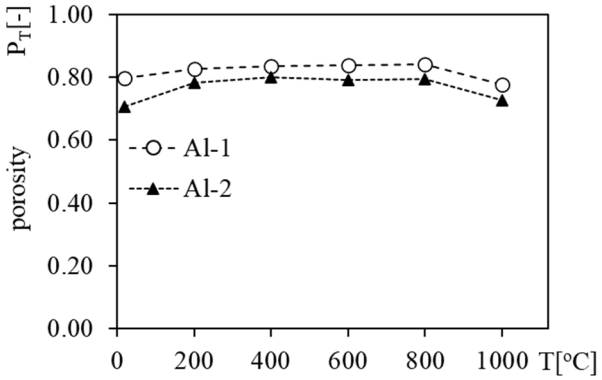

Figure 6. Porosity P of heated geopolymer foams Al-1 and Al-2 in the function of temperature.

The density (ρ) and apparent density (ρ_o) values enabled the total porosity determination (P). Porosity was calculated from the equation $P = 1 - (\rho_o/\rho)$. The evolution of total porosity P with temperature is represented in Figure 6 and shows the stable behaviour of geopolymer foams from coal gangue with temperature increase, positive aspect in case of fire-resistant material. The constant level of porosity, 83% and 78% at 200 °C, remained unchanged up to 800 °C. The stable porosity level in the whole range of tested temperatures ensured constant thermal insulation parameters with increasing temperature, which is extremely important for fire protection.

3.3. Mechanical Properties Evolution with Temperature

The mineral foams with apparent densities similar to the tested ones (600 and 800 kg/m^3), for example, aerated concrete, present relatively high mechanical performance. The data presented by the Foamed Concrete Composition and Properties, British Cement Association give the range of values 1.0–1.5 and 1.5–2.0 MPa in compression for densities of 600 and 800 kg/m^3. In Figure 7, absolute values of compressive strength in MPa and relative values of compressive strength f_{cT}/f_{c20} [-] were presented. Relative value refers to the compressive strength of the material (f_{cT}) heated to temperature T related to the reference strength of unheated material (f_{c20}). As presented in Figure 7, foams Al-1 and Al-2 presented mean values of compressive strength of 1.30 MPa and 3.30 MPa, respectively, at room temperature. This was higher than the levels reached by the aerated concretes.

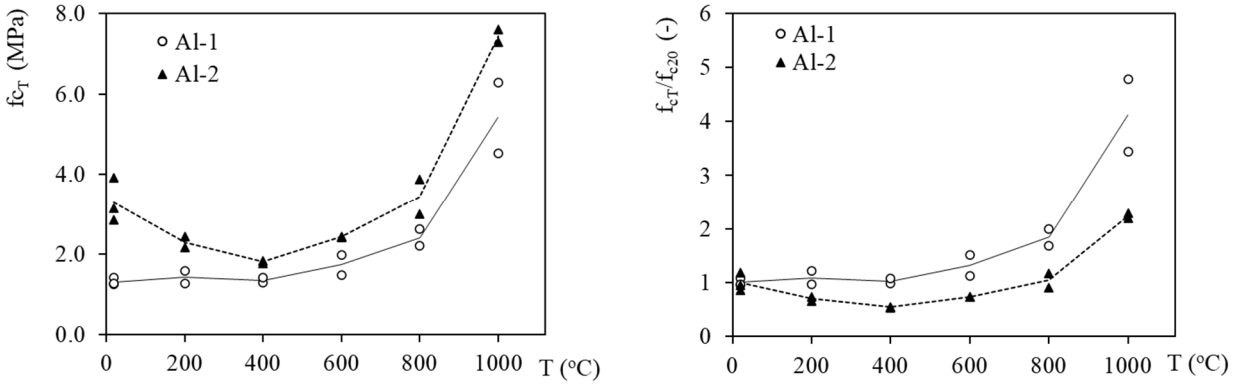

Figure 7. Compressive strength of heated geopolymer foams: absolute values in MPa and relative f_{cT}/f_{c20} values [-].

For Al-1 geopolymer foam, the compressive strength remained almost unchangeable up to 400 °C when compressive strength started to increase. The Al-2 foam, after exposition

at 200 °C and 400 °C, a decrease of mechanical performances in compression was observed. The first change is usually connected to dehydration [6,12,13,19]. This process causes a decrease in mechanical properties [6,12,13]. The tests of mechanical properties for Al-2 heated to 200 °C and 400 °C presented approximately 20% and 30% decrease in strength. To investigate the possible reasons for this reduction, SEM observations were undertaken. The SEM observation confirmed a more significant number of cracks in the material heated to 200 °C and 400 °C.

Nevertheless, similar to Al-1, progressive strength regain was observed with higher exposure temperatures. The essential strength growth due to sintering was noted for Al-1. The mean values of compressive strength at 800 °C and 1000 °C were 2.4 MPa and 5.4 MPa, which represents a relative increase of almost 2- and 4-fold. The microstructure of foams' matrices presented a dense, sintered and vitreous structure.

At temperature range 550–850 °C, for many geopolymers and their composites, significant shrinkage is observed [19,35,36]. It can be observed under a microscope as a structure with fewer voids and a smoother texture [19,37–39]. At this temperature, densification by vitreous sintering of the geopolymer matrix causes changes in microstructure [19,22,39]. Additionally, this kind of structure leads to crack healing [40]. In the case of investigated materials, the obtained results showed the possibility of occurrence of this mechanism at a temperature of approximately 800 °C with a slight increase of mechanical properties and caused the first change in microstructure. At 600 °C, these changes were not observed, and the microstructure was similar to that at lower temperatures.

Material that does not present a sharp strength decrease when heated can be considered a suitable characteristic for fire-resistant material used as a thermal barrier.

The flexural strength values evolution with temperature for the two tested geopolymer foams is presented in Figure 8. The reference values (20 °C) of tensile strength tested in three-point bending of Al-1 and Al-2 were 0.58 MPa and 1.71. Figure 8 presents the evolution of absolute values of flexural tensile strength in MPa and relative values of f_{tT}/f_{t20} [-]. Relative value refers to the tensile strength of the material (f_{tT}) heated to temperature T related to the reference strength of unheated material (f_{t20}). The evolution of tensile strength with temperature follows a similar pattern for both tested foams.

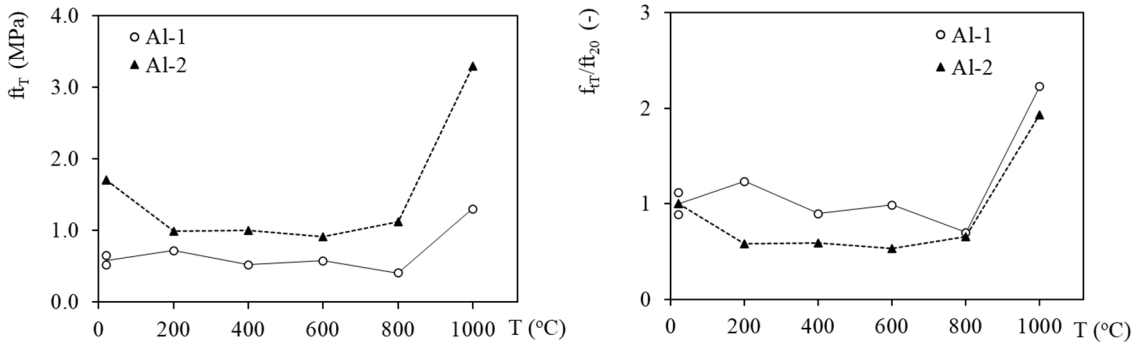

Figure 8. Tensile strength of heated geopolymer foams: absolute values in MPa and relative f_{tT}/f_{t20} values [-].

It was observed that mechanical behaviour in tension remains quasi-identical for the temperatures 200–800 °C. This was a positive aspect of the developed materials. Their mechanical behaviour was favourable for thermal barriers.

3.4. Microstructure Investigation with the Use of a Scanning Electron Microscope (SEM) and Chemical Composition

To explain the observed changes in mechanical and physical properties, microstructure was investigated using a scanning electron microscope (SEM). Unheated, as well as heated, samples were investigated to target temperature (Figures 9 and 10). The pictures were taken

at different magnifications to illustrate changes in the material structure and phenomena connected with exposure to high temperature.

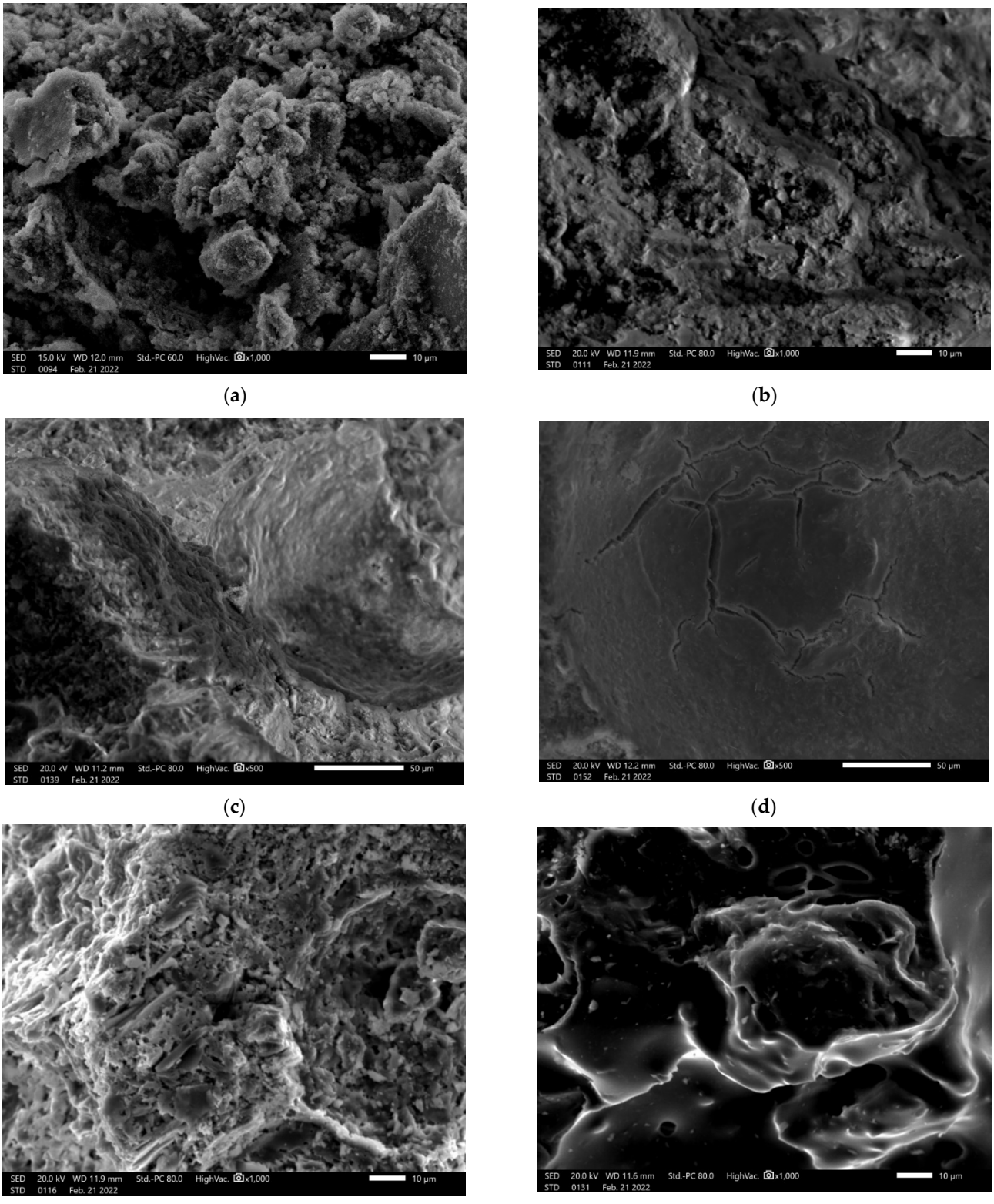

Figure 9. Microstructure of the Al-1 samples after exposure to temperature: (**a**) 20 °C Al-1; ×1000; (**b**) 200 °C Al-1; ×1000; (**c**) 400 °C Al-1; ×500; (**d**) 600 °C Al-1; ×500; (**e**) 800 °C Al-1; ×1000; (**f**) 1000 °C Al-1; ×1000.

Figure 9 shows the microstructure for the Al-1 samples. The microstructure observed in the temperature range between 20 °C and 400 °C was quite similar. At 400–600 °C, some cracks are visible (Figure 9d). After heating to 800 °C, the sintering process and vitreous structure appear (Figure 9e). The structure of the samples exposed at 1000 °C was quite different (Figure 9f). It is characterised by large glassy areas. The particular phases in the material were partially melted, which explains the increase in the mechanical performances (f_c and f_t). To supplement the information, energy dispersive spectroscopy (EDS) analysis was provided for the whole selected areas presented in Figure 9 to compare the oxide composition for the Al-1. The results are presented in Table 4.

Table 4. Comparison of the oxide composition of samples Al-1 based on EDS measurements from the surface presented in SEM pictures.

Oxide	20 °C	200 °C	400 °C	600 °C	800 °C	1000 °C
Na_2O	44.86 ± 0.17	23.20 ± 0.11	15.14 ± 0.11	12.39 ± 0.10	13.16 ± 0.10	10.13 ± 1.08
MgO	0.75 ± 0.04	1.39 ± 0.04	1.40 ± 0.04	1.37 ± 0.04	2.18 ± 0.04	1.81 ± 0.04
Al_2O_3	15.22 ± 0.13	18.54 ± 0.12	19.65 ± 0.12	20.29 ± 0.13	20.38 ± 0.13	23.86 ± 1.53
SiO_2	36.84 ± 0.21	50.27 ± 0.21	58.36 ± 0.23	59.74 ± 0.25	55.02 ± 0.22	55.01 ± 2.58
K_2O	2.34 ± 0.05	2.21 ± 0.04	1.88 ± 0.03	2.23 ± 0.04	2.21 ± 0.04	2.65 ± 0.46
FeO	4.41 ± 0.20	4.39 ± 0.10	3.58 ± 0.07	3.97 ± 0.08	6.43 ± 0.09	6.35 ± 1.21

The oxide composition presented in Table 4 is typical for geopolymer material. Taking into account the qualitative character of this type of investigation, there were no significant differences between materials exposed at different temperatures. The dominant oxides are silicon dioxide and aluminium oxide. In the composition, we observed that there was no CaO in the geopolymer structure. SiO_2 and Al_2O_3 build the main structure of the material. The important compound is sodium oxide. It plays an important role in the geopolymerisation process [1]. As the temperature decreased, the amount of sodium oxide decreased. It could be the effect of the qualitative characteristics of the method (selection of the area where sodium oxide was not fully reacted) or the decomposition of this compound that has a place in the temperature of approximately 600 °C [41]. In addition, the amount of sodium oxide decreased with increasing temperatures. The amount of iron oxide increased. The existence of iron in this composition caused the reddish colour of the material obtained. The presence of iron is usually considered an advantage in the geopolymerisation process [42]. It is a high probability that a large amount of this oxide appeared at a temperature higher than 800 °C. The confirmation of this phenomenon is also the change in colour of the samples exposed at 800 °C and 1000 °C, as FeO has a dark colour (usually black) compared to other iron compounds, for example, Fe_2O_3 that has a red colour. Other oxides, such as potassium and magnesium, appear in low amounts and their amount is more or less stable.

The results obtained for Al-1 were compared with the results obtained for Al-2. The microstructure of these samples is presented in Figure 10.

Similar to Al-1 samples, the microstructure of samples Al-2 in the temperature range between 20 °C and 600 °C is typical for geopolymer structures [43,44]. In the case of the samples exposed at the temperature of 800 °C, the vitreous sintered structure was observed, which is presented on the left side in Figure 10f. After exposition to 1000 °C, most of the structures presented a glassy phase, and the material structure was significantly different than at lower temperatures (Figure 10). Above the temperature 850 °C, the crystallisation of geopolymers is observed [19,45]. For the investigated materials, an increase in mechanical properties was noticed, and clear changes in microstructure were observed. Some previous investigation shows similar phenomena for metakaolin-based geopolymers, where loses its strength up to 800 °C due to dehydroxylation, have displayed a strength gain at over 1000 °C due to sintering [22,46]. A similar phenomenon was observed on waste clays [43] and geopolymers with additional silica fume [47]. Other investigation shows the possibility of changing the porous structure in the material that

caused structure reinforcement [48] or, in some cases, decreasing the mechanical properties due to intensive cracking [19,45]. Bai et al. [49] reported that for porous geopolymers containing a large amount of waste glass in the temperature range 700–900 °C, an effect of secondary foaming. In our investigation, we did not notice such behaviour.

Furthermore, for the selected areas, the oxide composition of Al-2 was provided (Table 5), corresponding to the selected areas presented in Figure 10.

Table 5. Comparison of the oxides composition based on EDS of Al-2 from the surface presented on SEM pictures.

Oxide	20 °C	200 °C	400 °C	600 °C	800 °C	1000 °C
Na_2O	17.97 ± 0.11	12.57 ± 0.17	7.55 ± 0.10	13.27 ± 0.24	9.90 ± 0.12	10.09 ± 0.18
MgO	1.33 ± 0.03	1.74 ± 0.07	1.91 ± 0.05	1.11 ± 0.08	1.19 ± 0.05	1.12 ± 0.07
Al_2O_3	17.11 ± 0.11	19.57 ± 0.21	20.51 ± 0.16	18.88 ± 0.27	23.20 ± 0.18	23.08 ± 0.25
SiO_2	56.41 ± 0.21	56.38 ± 0.39	61.62 ± 0.30	52.30 ± 0.49	56.99 ± 0.31	53.01 ± 0.43
K_2O	1.68 ± 0.03	2.83 ± 0.07	3.37 ± 0.06	2.66 ± 0.09	4.10 ± 0.07	4.55 ± 0.10
TiO_2	0.99 ± 0.03	—	—	1.31 ± 0.09	—	—
FeO	4.51 ± 0.07	6.92 ± 0.17	5.03 ± 0.11	10.47 ± 0.27	4.62 ± 0.11	8.17 ± 0.21

The results obtained for the oxide composition for the Al-2 samples are quite similar to those of the Al-1 samples. This was expected because for both compositions, the same raw material was applied. The dominant oxides were silicon dioxide and aluminium oxide. The double aluminium portion used in the preparation process did not influence the amount of aluminium in the oxide composition of the investigated samples.

In the composition, we observed that CaO was not present in the geopolymer structure. In the ambient temperature and the samples exposed at the temperature 600 °C, titanium dioxide appeared in this composition, but the amount was small, and it should be treated as impurities that come from raw material. The overall tendency was coherent with decreasing amounts of sodium oxide and increasing amounts of iron oxide with the temperature; however, there was some incoherence for 800 °C that should be treated as imperfections of the used method of analysis that has a qualitative character.

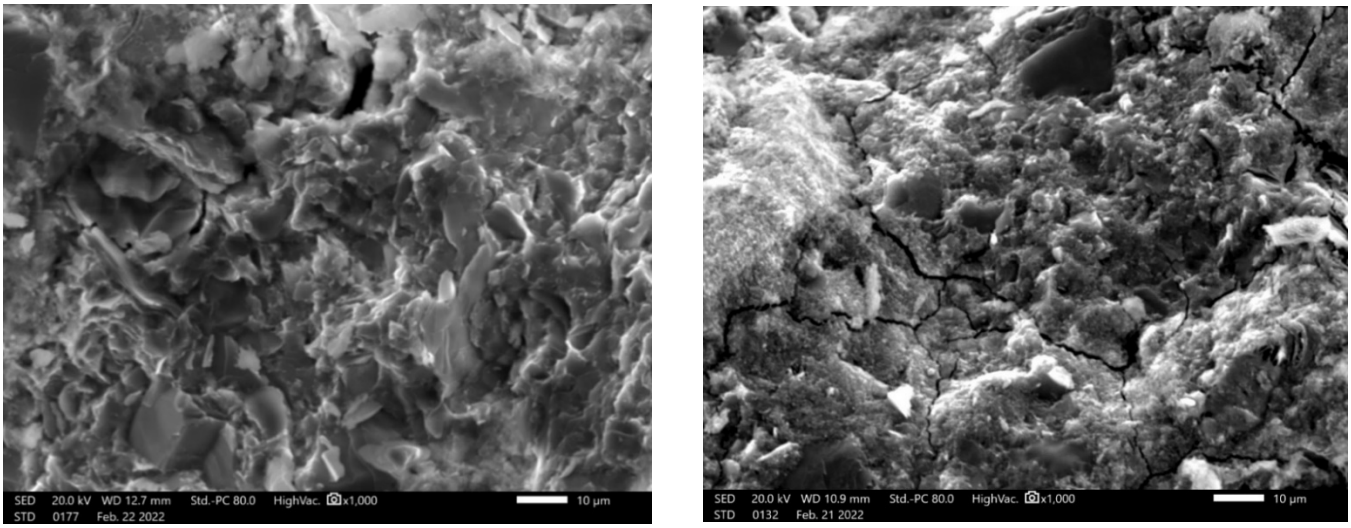

(**a**) (**b**)

Figure 10. *Cont.*

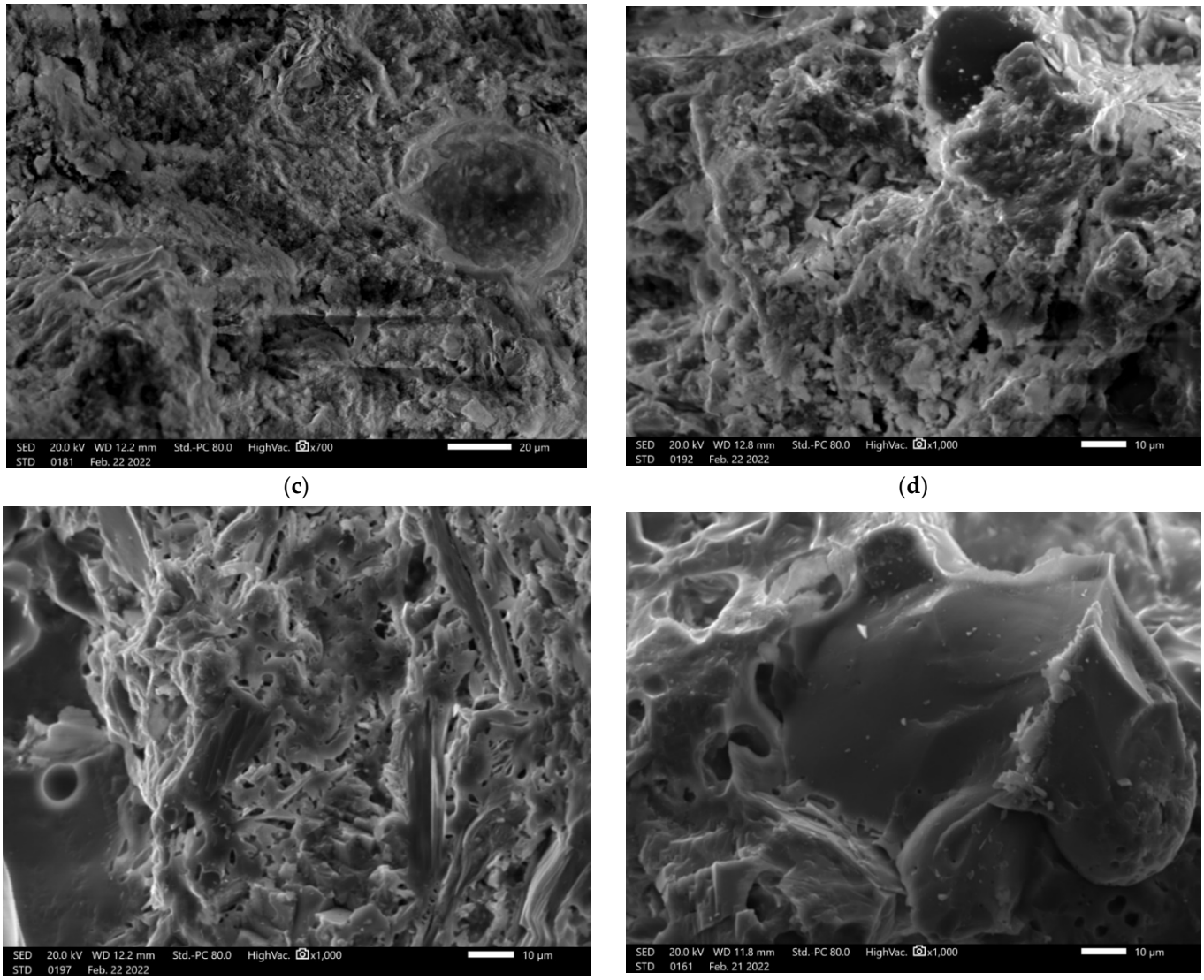

Figure 10. Microstructure of the samples Al-2 after exposure to temperature: (**a**) 20 °C Al-2; ×1000; (**b**) 200 °C Al-2; ×1000; (**c**) 400 °C Al-2; ×700; (**d**) 600 °C Al-2; ×1000; (**e**) 800 °C Al-2; ×1000; (**f**) 1000 °C Al-2; ×1000.

The other possible explanation for the reinforcement mechanism is transit to metakaolinite into Al–Si spinel and mullite [50]. This phenomenon should be confirmed by other research. The temperature resistance of geopolymers is an advantage, which is indicated by numerous literature reports [3,6,9,31–33,51,52].

To provide a more extensive analysis of the results, the diffractograms of crystalline phases XRD present in unheated geopolymer foam A1-1 (20 °C) and heated to 1000 °C were provided. This enabled the comparison of phases present in the geopolymer foam matrix before and after heating. In unheated material, muscovite (39.5%), quartz (34.1%), albite (22.6%) and mullite (3%) were present. After heating to 1000 °C the mullite amount increased significantly, reaching a level of 37.7%, which is in agreement with the literature observations [50]. The other components were quartz (33.6%), albite (27.4%) and muscovite (1.4%) (Figures 11 and 12).

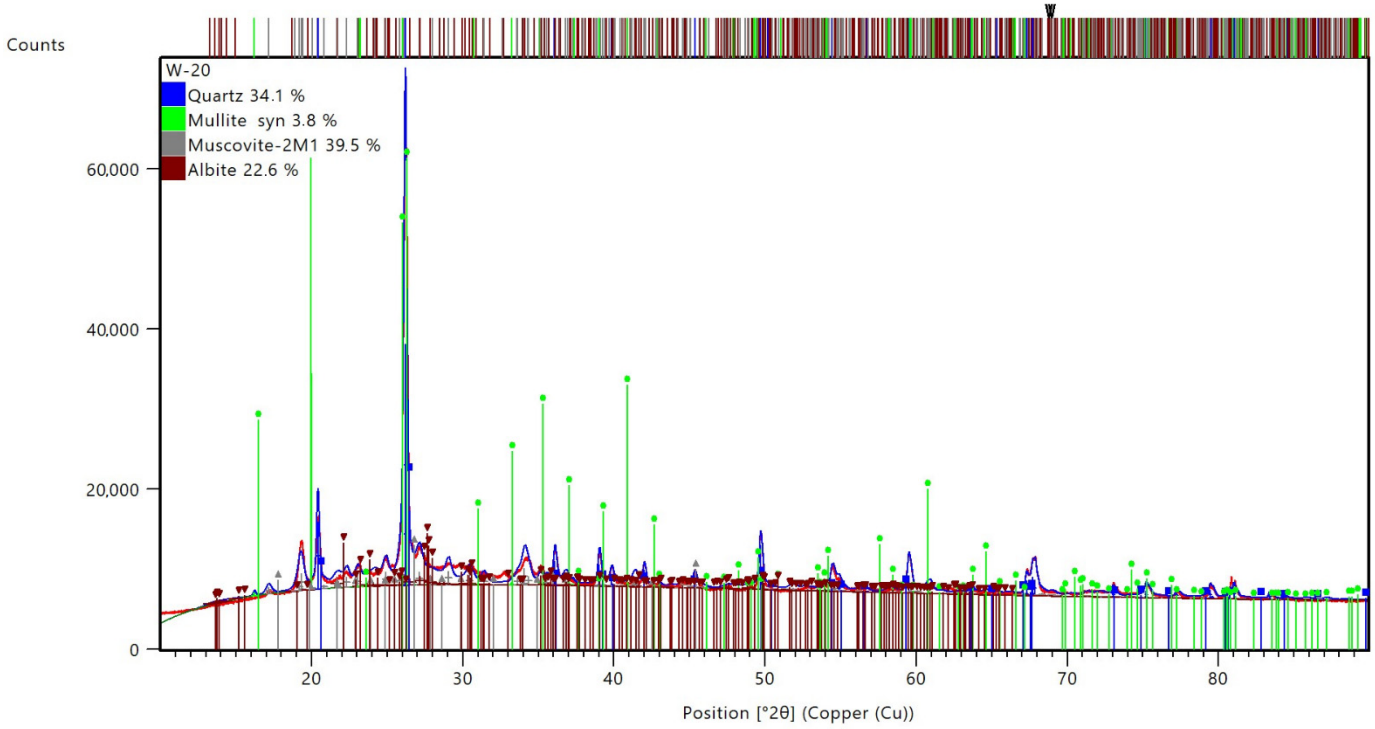

Figure 11. XRD of unheated coal gangue geopolymer foam A1-1 (20 °C).

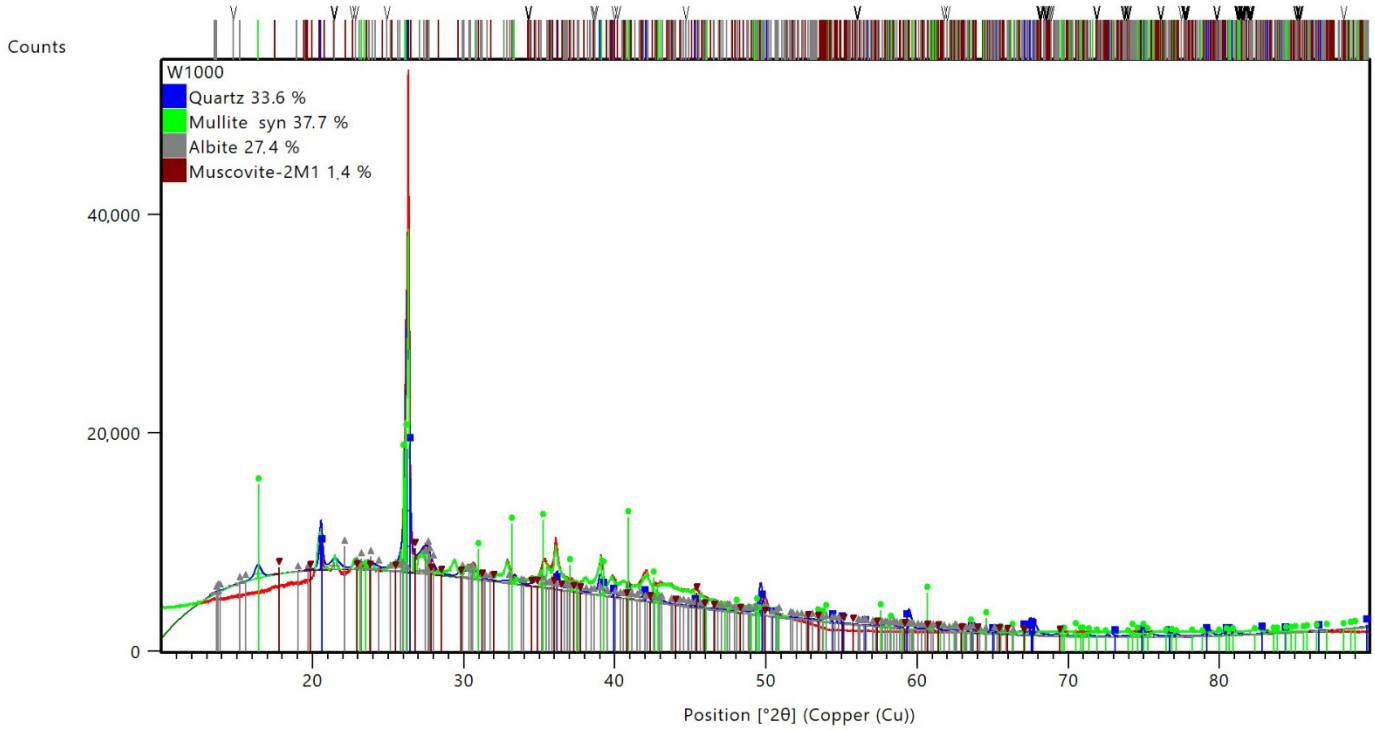

Figure 12. XRD of heated to 1000°C coal gangue geopolymer foam A1-1.

4. Conclusions

In the present research, the possibility of coal waste management was investigated. The main task was to verify whether the coal gangue composition from the Wieczorek mine was adequate for geopolymer synthesis. Coal gangue composition was identified as quartz 50% and kaolinite (30%) and this aluminosilicate is potentially adequate for use as a precursor in geopolymer synthesis. As research has shown, precursor activation with

the presence of aluminium powder and hydrogen peroxide enabled the manufacturing of foamed geopolymers. With two levels of aluminium powder addition, stable foams were produced with porosities of 80 and 70% for Al-1 and Al-2. Surprisingly, the higher level of foaming agent (Al-2) did not ensure higher porosity but only influenced its type, resulting in smaller pores evenly distributed in the material.

Heating in the range of temperatures up to 1000 °C did not affect the total porosity of tested foams. At the whole temperature range, the porosity of Al-1 and Al-2 remained practically unchanged. This is considered a favourable feature of developed material, resulting in stable thermal insulation potential. Moreover, geopolymer foams based on coal gangue present stable mechanical properties in the range of tested temperatures. No sharp mechanical performances decreased, and no spalling events or material chipping was observed. Al-1 and Al-2 tensile strengths were 0.58 MPa and 1.71, respectively, and remained quasi-identical for temperatures in range 200–800 °C. This is a positive aspect of the developed materials. Their mechanical behaviour is favourable for thermal barriers.

Al-1 and Al-2 presented mean values of compressive strength of 1.30 MPa and 3.30 MPa at room temperature. Due to sintering and the mullite amount increase from 3% at 20 °C to the level of 37.7% at 1000 °C, confirmed by XRD tests, the mechanical performances significantly increased the values of compressive strength at 1000 °C increased. The values of 5.40 MPa and 7.30 MPa, respectively, for Al-1 and Al-2 were noted, which represents a relative increase of almost 2- and 4-fold.

No spalling or chipping was observed after heating. The total porosity at 200 °C (83% and 78% for Al-1 and Al-2) remained unchanged up to 800 °C. The stable porosity level in the whole range of tested temperatures ensures constant thermal insulation parameters at high temperatures, which is extremely important for fire protection. The colour change of heated samples occurred and was explained by the iron oxidation of ferrous components, which does not affect overall material behaviour and suitability as a thermal barrier.

The developed material from alkali-activated coal gangue is an exciting possibility for coal mine waste management. In particular, the foamed nature of the geopolymer offers many possibilities for the implementation of thermal barriers to protect against fire. Foamed geopolymer composites can be highly positioned at the scale of materials, enabling efficient management of mining waste materials, which is essential to building a culture of sustainability and developing the circular economy concept.

Author Contributions: Conceptualisation, I.H., K.K., J.C.-G. and M.S.; methodology, M.S.; validation, I.H., M.Ł., J.C.-G. and M.S.; formal analysis, K.M. and J.C.-G.; investigation, B.F., M.S., K.K., M.Ł. and K.M.; data curation, B.F., M.S. and K.M.; writing—original draft preparation, B.F., K.K. and I.H.; writing—review and editing, I.H., M.Ł., J.C.-G., M.S. and K.M.; visualisation, M.S.; supervision, I.H.; project administration, I.H.; funding acquisition, K.K., I.H. and J.C.-G. All authors have read and agreed to the published version of the manuscript.

Funding: This work was financed by the Polish National Agency for Academic Exchange under the International Academic Partnership Program within the framework of the grant: E-mobility and sustainable materials and technologies EMMAT (PPI/APM/2018/1/00027). This work was partially financed by the NCBR and EU in framework of the project SMART-G Smart geopolymers ERA-MIN2-3/SMART-G/1/2022.

Institutional Review Board Statement: Not applicable.

Informed Consent Statement: Not applicable.

Data Availability Statement: Not applicable.

Acknowledgments: The research was part of the work provided by an interdisciplinary research group: 'Geopolymer composites for construction' (GEOMAT).

Conflicts of Interest: The authors declare no conflict of interest. The funders had no role in the design of the study; in the collection, analyses, or interpretation of data; in the writing of the manuscript, or in the decision to publish the results.

References

1. Davidovits, J. 30 Years of Successes and Failures in Geopolymer Applications. Market Trends and Potential Breakthroughs. In Proceedings of the Geopolymer 2002 Conference, Melbourne, VIC, Australia, 28–29 October 2002. Available online: https://www.geopolymer.org/wp-content/uploads/30YearsGEOP.pdf (accessed on 1 March 2022).
2. Łach, M. Geopolymer Foams—Will They Ever Become a Viable Alternative to Popular Insulation Materials?—A Critical Opinion. *Materials* **2021**, *14*, 3568. [CrossRef] [PubMed]
3. Amran, M.; Huang, S.S.; Debbarma, S.; Rashid, R.S.M. Fire resistance of geopolymer concrete: A critical review. *Constr. Build. Mater.* **2022**, *324*, 126722. [CrossRef]
4. Łach, M.; Korniejenko, K.; Mikuła, J. Thermal Insulation and Thermally Resistant Materials Made of Geopolymer Foams. *Procedia Eng.* **2016**, *151*, 410–416. [CrossRef]
5. Korniejenko, K.; Figiela, B.; Ziejewska, C.; Marczyk, J.; Bazan, P.; Hebda, M.; Choińska, M.; Lin, W.-T. Fracture Behavior of Long Fiber Reinforced Geopolymer Composites at Different Operating Temperatures. *Materials* **2022**, *15*, 482. [CrossRef] [PubMed]
6. Lahoti, L.; Hai Tan, K.; Yang, E.H. A critical review of geopolymer properties for structural fire-resistance applications. *Constr. Build. Mater.* **2019**, *221*, 514–526. [CrossRef]
7. Kozub, B.; Bazan, P.; Gailitis, R.; Korniejenko, K.; Mierzwiński, D. Foamed Geopolymer Composites with the Addition of Glass Wool Waste. *Materials* **2021**, *14*, 4978. [CrossRef]
8. Kong, D.L.Y.; Sanjayan, J.G.; Sagoe-Crentsil, K. Comparative performance of geopolymers made with metakaolin and fly ash after exposure to elevated temperatures. *Cem. Concr. Res.* **2007**, *37*, 1583–1589. [CrossRef]
9. Le, V.S.; Louda, P.; Tran, H.N.; Nguyen, P.D.; Bakalova, T.; Ewa Buczkowska, K.; Dufkova, I. Study on Temperature-Dependent Properties and Fire Resistance of Metakaolin-Based Geopolymer Foams. *Polymers* **2020**, *12*, 2994. [CrossRef]
10. Shaikh, F.; Haque, S. Behaviour of Carbon and Basalt Fibres Reinforced Fly Ash Geopolymer at Elevated Temperatures. *Int. J. Concr. Struct. Mater.* **2018**, *12*, 35. [CrossRef]
11. Zhang, H.-Y.; Hao, X.; Fan, W. Experimental Study on High Temperature Properties of Carbon Fiber Sheets Strengthened Concrete Cylinders Using Geopolymer as Adhesive. *Procedia Eng.* **2016**, *135*, 47–55. [CrossRef]
12. Behera, P.; Baheti, V.; Militky, J.; Naeem, S. Microstructure and mechanical properties of carbon microfiber reinforced geopolymers at elevated temperatures. *Constr. Build. Mater.* **2018**, *160*, 733–743. [CrossRef]
13. Behera, P.; Baheti, V.; Militky, J.; Louda, P. Elevated temperature properties of basalt microfibril filled geopolymer composites. *Constr. Build. Mater.* **2018**, *163*, 850–860. [CrossRef]
14. Celik, A.; Yilmaz, K.; Canpolat, O.; Al-Mashhadani, M.M.; Aygörmez, Y.; Uysal, M. High-temperature behavior and mechanical characteristics of boron waste additive metakaolin based geopolymer composites reinforced with synthetic fibers. *Constr. Build. Mater.* **2018**, *187*, 1190–1203. [CrossRef]
15. Alomayri, T.; Shaikh, F.; Low, I.M. Characterisation of cotton fibre-reinforced geopolymer composites. *Compos. Part B Eng.* **2013**, *50*, 1–6. [CrossRef]
16. Alomayri, T.; Shaikh, F.; Low, I. Mechanical and thermal properties of ambient cured cotton fabric-reinforced fly ash-based geopolymer composites. *Ceram. Int.* **2014**, *40*, 14019–14028. [CrossRef]
17. Constancio Trindade, A.C.; Alcamand, H.A.; Ribeiro Borges, P.H.; de Andrade Silva, F. Influence of Elevated Temperatures on the Mechanical Behavior of Jute-Textile-Reinforced Geopolymers. *J. Ceram. Sci. Technol.* **2017**, *8*, 389–398.
18. Tayeh, B.A.; Zeyad, A.M.; Agwa, I.S.; Amin, M. Effect of elevated temperatures on mechanical properties of lightweight geopolymer concrete. *Case Stud. Constr. Mater.* **2021**, *15*, e00673. [CrossRef]
19. Nodehi, M. A comparative review on foam-based versus lightweight aggregate-based alkali-activated materials and geopolymer. *Innov. Infrastruct. Solut.* **2021**, *6*, 231. [CrossRef]
20. Ali, M.F.; Natrajan, M.M.V. A Review of Geopolymer Composite Thermal Properties. *IOP Conf. Ser. Earth Environ. Sci.* **2021**, *822*, 012051. [CrossRef]
21. Cheng-Yong, H.; Yun-Ming, L.; Al Bakri Abdullah, M.M.; Hussin, K. Thermal Resistance Variations of Fly Ash Geopolymers: Foaming Responses. *Sci. Rep.* **2017**, *7*, 45355. [CrossRef]
22. Dhasindrakrishna, K.; Pasupathy, K.; Ramakrishnan, S.; Sanjayan, J. Progress, current thinking and challenges in geopolymer foam concrete technology. *Cem. Concr. Compos.* **2021**, *116*, 103886. [CrossRef]
23. Zhang, Z.; Provis, J.L.; Reid, A.; Wang, H. Mechanical, thermal insulation, thermal resistance and acoustic absorption properties of geopolymer foam concrete. *Cem. Concr. Compos.* **2015**, *62*, 97–105. [CrossRef]
24. Duan, P.; Song, L.; Yan, C.; Ren, D.; Li, Z. Novel thermal insulating and lightweight composites from metakaolin geopolymer and polystyrene particles. *Ceram. Int.* **2017**, *43*, 5115–5120. [CrossRef]
25. Teng, N.H.; Cheng-Yong, H.; Yun-Ming, L.; Al Bakri Abdullah, M.M.; Hussin, K. The Mechanical Properties and Thermal Resistance of Fly Ash Geopolymer Foams. *Solid State Phenom.* **2018**, *281*, 175–181. [CrossRef]
26. Le, V.S.; Szczypinski, M.M.; Hájková, P.; Kovacic, V.; Bakalova, T.; Volesky, L.; Hiep, L.C.; Louda, P. Mechanical properties of geopolymer foam at high temperature. *Sci. Eng. Compos. Mater.* **2020**, *27*, 129–138. [CrossRef]
27. PN-EN 1008:2017. Mixing Water for Concrete—Specification for Sampling, Testing and Assessing the Suitability of Water, Including Water Recovered from Processes in the Concrete Industry, As Mixing Water for Concrete. Available online: https://standards.iteh.ai/catalog/standards/cen/8ab1a0fa-b727-48f7-9b31-739eba3732ca/en-1008-2002 (accessed on 25 March 2022). (In Polish)

28. Kastiukas, G.; Zhou, X.; Wan, K.T.; Castro-Gomes, J. Lightweight alkali-activated material from mining and glass waste by chemical and physical Foaming. *J. Mater. Civ. Eng.* **2019**, *31*, 04018397. [CrossRef]
29. Szechyńska-Hebda, M.; Marczyk, J.; Ziejewska, C.; Hordyńska, N.; Mikuła, J.; Hebda, M. Optimal design of pH-neutral geopolymer foams for their use in ecological plant cultivation systems. *Materials* **2019**, *12*, 2999. [CrossRef]
30. Schneider, U.; Felicetti, R.; Debicki, G.; Diederichs, U.; Franssen, J.M.; Jumppanen, U.M.; Khoury, G.A.; Leonovich, S.; Millard, A.; Morris, W.A.; et al. Recommendation of RILEM TC 200-HTC: Mechanical concrete properties at high temperatures-modelling and applications: PGeneral presentation. *Mater. Struct. Constr* **2007**, *40*, 841–853. [CrossRef]
31. Hager, I.; Sitarz, M.; Mróz, K. Fly-ash based geopolymer mortar for high-temperature application—Effect of slag addition. *J. Clean. Prod.* **2021**, *316*, 128168. [CrossRef]
32. Dudek, M.; Sitarz, M. Analysis of changes in the microstructure of geopolymer mortar after exposure to high temperatures. *Materials* **2020**, *13*, 4263. [CrossRef]
33. Hager, I.; Sitarz, M.; Mróz, K. Behaviour of fly ash geopolymer at high temperature. In Proceedings of the 2020 5th International Conference on Smart and Sustainable Technologies (SpliTech), Split, Croatia, 23–26 September 2020.
34. Hager, I. Colour change in heated concrete. *Fire Technol.* **2014**, *50*, 945–958. [CrossRef]
35. Pantongsuk, T.; Kittisayarm, P.; Muenglue, N.; Benjawan, S.; Thavorniti, P.; Tippayasam, C.; Nilpairach, S.; Heness, G.; Chaysuwan, D. Effect of hydrogen peroxide and bagasse ash additions on thermal conductivity and thermal resistance of geopolymer foams. *Mater. Today Commun.* **2021**, *26*, 102149. [CrossRef]
36. Kong, D.L.Y.; Sanjayan, J.G.; Sagoe-Crentsil, K. Factors affecting the performance of metakaolin geopolymers exposed to elevated temperatures. *J. Mater. Sci.* **2008**, *43*, 824–831. [CrossRef]
37. Nicoara, A.I.; Badanoiu, A.; Balanoiu, M.; Mathias, A.; Voicu, G. Alkali Activated Mortars with Intumescent Properties. *Rev. Chim.* **2019**, *70*, 431–437. [CrossRef]
38. Luo, Y.; Li, S.H.; Klima, K.M.; Brouwers, H.J.H.; Yu, O. Degradation mechanism of hybrid fly ash/slag based geopolymers exposed to elevated temperatures. *Cem. Concr. Res.* **2022**, *151*, 106649. [CrossRef]
39. Liu, H.; Jing, W.; Qin, L.; Duan, P.; Zhang, Z.; Guo, R.; Li, W. Thermal stability of geopolymer modified by different silicon source materials prepared from solid wastes. *Constr. Build. Mater.* **2022**, *315*, 125709. [CrossRef]
40. Lahoti, M.; Wong, K.K.; Tan, K.H.; Yang, E.H. Effect of alkali cation type on strength endurance of fly ash geopolymers subject to high temperature exposure. *Mater. Des.* **2018**, *154*, 8–19. [CrossRef]
41. Kumara, R.; Miyaoka, H.; Shinzato, K.; Ichikawa, T. Analysis of sodium generation by sodium oxide decomposition on corrosion resistance materials: A new approach towards sodium redox water-splitting cycle. *RSC Adv.* **2021**, *11*, 21017–21022. [CrossRef]
42. Obonyo, E.A.; Kamseu, E.; Lemougna, P.N.; Tchamba, A.B.; Melo, U.C.; Leonelli, C. A Sustainable Approach for the Geopolymerization of Natural Iron-Rich Aluminosilicate Materials. *Sustainability* **2014**, *6*, 5535–5553. [CrossRef]
43. Zawrah, M.F.; Sadek, H.E.H.; Ngida, R.E.A.; Abo Sawan, S.E.; El-Kheshen, A.A. Effect of low-rate firing on physico-mechanical properties of unfoamed and foamed geopolymers prepared from waste clays. *Ceram. Int.* **2022**, *48*, 11330–11337. [CrossRef]
44. Choi, Y.C.; Park, B. Effects of high-temperature exposure on fractal dimension of fly-ash-based geopolymer composites. *J. Mater. Res. Technol.* **2020**, *9*, 7655–7668. [CrossRef]
45. Klima, K.M.; Schollbach, K.; Brouwers, H.J.H.; Yu, O. Thermal and fire resistance of Class F fly ash based geopolymers—A review. *Constr. Build. Mater.* **2022**, *323*, 126529. [CrossRef]
46. Cilla, M.S.; de Mello Innocentini, M.D.; Morelli, M.R.; Colombo, P. Geopolymer foams obtained by the saponification/peroxide/gelcasting combined route using different soap foam precursors. *J. Am. Ceram. Soc.* **2017**, *100*, 3440–3450. [CrossRef]
47. Abo Sawan, S.E.; Zawrah, M.F.; Khattab, R.M.; Abdel-Shafi, A.A. In-situ formation of geopolymer foams through addition of silica fume: Preparation and sinterability. *Mater. Chem. Phys.* **2020**, *239*, 121998. [CrossRef]
48. Yan, S.; Zhang, F.; Feng, X.; Kong, J.; Wang, B.; Yang, J. Effect of high temperature on the mechanical properties of hierarchical porous cenosphere/geopolymer composite foams. *Int. J. Appl. Ceram. Technol.* **2021**, *18*, 817–829. [CrossRef]
49. Bai, C.; Li, H.; Bernardo, E.; Colombo, P. Waste-to-resource preparation of glass-containing foams from geopolymers. *Ceram. Int.* **2019**, *45*, 7196–7202. [CrossRef]
50. Chen, Y.F.; Wang, M.C.; Hon, M.H. Phase transformation and growth of mullite in kaolin ceramics. *J. Eur. Ceram. Soc.* **2004**, *24*, 2389–2397. [CrossRef]
51. Luhar, S.; Nicolaides, D.; Luhar, I. Fire Resistance Behaviour of Geopolymer Concrete: An Overview. *Buildings* **2021**, *11*, 82. [CrossRef]
52. Zhang, Z.; Provis, J.L.; Reid, A.; Wang, H. Geopolymer foam concrete: An emerging material for sustainable construction. *Constr. Build. Mater.* **2014**, *56*, 113–127. [CrossRef]